

## **Wavelet analysis identifies geology in seismic**

Geologic lithofacies can be quantitatively identified by the wavelet decomposition of the seismic reflection. That is, the reservoir risk can be mitigated by a quantitative estimation of its probability. The method appears to be robust, working on data that would not support conventional amplitude analysis. Geology with a dominant bed thickness and spacing, requiring 60 Hz seismic to resolve, can be easily identified with 10 Hz seismic. A byproduct of this technology development was the discovery of the superiority of discrete wavelet transform methods over Fourier techniques in deconvolution of the seismic signal, needed for lithofacies identification.

The fundamental concept behind this analysis is shown in Fig. 1. The reflection of a seismic pressure pulse off a seismic reflector imprints the “color” of the geologic beds on the reflected pressure pulse. This “color” can then be used to identify the geology. This is a dramatic departure from the conventional view of the reflection of seismic off step acoustic impedance contrasts. A pulse reflected off such a profile will have exactly the same shape, and therefore “color”, as the incident pulse. This view simplifies things for conventional analysis but overlooks a piece of very useful information – the “color”.

The section of the acoustic impedance shown as the thin red line in Fig. 1 is a very complex signal. It is a localized burst that appears as a burst of reflected seismic pressure. This burst can be decomposed, taken apart, into its constituent parts by a wavelet transformation as shown in Fig. 2. The wavelet transformation shows the “color” of the well log’s acoustic impedance and the reflected seismic pressure pulse.

Two different geologic lithofacies are analyzed in Fig. 2. The acoustic impedance profiles, shown as the blue line next to the color images, is a very complex trace. The differences between the two lithofacies would be very difficult to discern given only these traces. The wavelet decompositions, shown as the color images next to the traces, are dramatically different. The color represents the amount of the signal at a particular depth for a particular bed thickness. It can be interpreted as a localized Fourier decomposition of the signal which tells how much of each frequency (inverse of bed thickness, spacing or scale) the signal has at each depth. Lithofacies A is the most complex. Near the top of the complex, it has predominately thick beds of the size indicated by the larger black bar shown on the impedance trace. One knows this by the existence of the red blob near the circle labeled **a**. This complex is more complicated near its base. The average bed thickness is indicated by the circle labeled **b**, and is displayed as the smaller black bar. It is only the average; there is quite a range of bed thickness indicated by the long tentacle of dark red near **b**. Lithofacies B is much simpler. It has a single predominate bed thickness that would take 60 Hz seismic to resolve.

This leads us to the critical question – what aspects of this “color” can be seen in the seismic reflection and how closely does it resemble the well log? The answer is shown in Fig. 2 as the wavelet decomposition of the seismic signal. There is a remarkable similarity between the well logs and the seismic. The main difference occurs at small scales and is due to the limited power in the seismic signal at these scales (the average frequency in the seismic data was 20 Hz). This is even more remarkable because of

quality of the seismic data. A gas amplitude anomaly, proven by the drill bit, was not seen on this data. It was seen on another dataset that had both superior acquisition and processing.

A very interesting aspect of this identification is the dominant frequency of the geologic bed thickness for lithofacies B – 60 Hz. The seismic data only had a dominant frequency of 20 Hz. Why is one able to restore these frequencies and tell the difference between the lithofacies? The reason is that one does not need to image the beds, that is place the beds accurately to within the bed thickness. One only needs to know that these beds exist within the complex of 200 m thickness. In technical terms, the instantaneous phase does not need to be known, only the magnitude. Making things even easier, the magnitude does not need to be placed accurately (only to within a 100 m or so). The phase coherency is the first thing to be destroyed in low quality data and at high frequency. The rough spectral magnitude is the last to be destroyed.

There is one technical aspect of the construction of the seismic wavelet spectrum that is a useful byproduct of this work – the processing needed to be done to the seismic data in order that it matched the well log data (a linear inversion, equivalent to deconvolution). A discrete wavelet transform method was used to do this. It was found to be superior to Fourier transform methods. It had a better signal to noise ratio (22 dB, compared to 14 dB), and more localized deconvolution artifacts. This finding has an important application to standard seismic processing. Deconvolution is an important part of standard processing. The current, widely used, methods are all based on Fourier

transforms. The performance of these algorithms would be improved by converting them to wavelet transform based approaches.

It is nice to be able to qualitatively see the difference in the lithofacies shown in Fig. 2, but the significant business value comes from qualitatively converting these differences into prospect reservoir risks. The fundamental information needed is a calibration database of well values for a relevant attribute of the wavelet transform. An example attribute is the dominant scale (geologic bed thickness) of the wavelet transform,  $\langle \mathbf{s} \rangle$ .

The probability distribution of observing this attribute given the lithofacies,

$P(\langle \mathbf{s} \rangle | \text{lithofacies})$ , is shown in Fig. 3. There are more than 10 independent samples from 14 wells for each lithofacies. There is significant separation in the populations.

To convert the conditional probabilities,  $P(\langle \mathbf{s} \rangle | \text{lithofacies})$ , to prospect risks,

$P(\text{lithofacies} | \langle \mathbf{s} \rangle)$ , a Bayesian inversion must be done. Given the observed wavelet transform of the seismic for lithofacies A (shown as the black circle labeled A in Fig. 3) one would estimate the probability of it being A to be 95%. The certainty of lithofacies B being B, given the wavelet transform of its seismic reflection (shown as the black circle labeled B in Fig. 3), is not as great. It is 77%. The prior probabilities of each lithofacies are assumed to be 50%. If one of the lithofacies was reservoir and the other was not, this would directly affect the expected net present value of prospects.

This work was supported by the BHP Billiton Petroleum technology program. Computer software to generate and view wavelet transformations is available under an Open Source

license agreement from: [http://www.int.com/products/java\\_toolkit\\_info/BHPViewer.htm](http://www.int.com/products/java_toolkit_info/BHPViewer.htm)  
and <http://www.cwp.mines.edu/cwpcodes/>.

Michael E. Glinsky and Jesse J. Melick  
BHP Billiton Petroleum, Houston, Texas, USA

Moshe Strauss and Micha Sapir  
Nuclear Research Center, Negev, Beer Sheva, Israel

For further information contact:

Michael E. Glinsky, Ph.D.  
BHP Billiton Petroleum  
1360 Post Oak Blvd., Suite 150  
Houston, TX 77056, USA  
email: [michael.e.glinsky@bhpbilliton.com](mailto:michael.e.glinsky@bhpbilliton.com)

## FIGURE CAPTIONS

**FIG. 1.** The pressure profile (thick blue line) and the derivative of the acoustic impedance profile (thin red line) shown in arbitrary units vs. depth for a time (a) before, (a) during, (b) after the reflection. The arrows indicate the direction of propagation of the pressure pulse.

**FIG. 2.** Well log acoustic impedance derivative vs. depth shown as the blue line graph on the right, wavelet transform plotted as the color image. (a) Lithofacies A, the part of the wavelet shown as the  $\alpha$  circle corresponds to beds of the size and location of the larger bar shown on the blue line graph, the  $\beta$  circle corresponds to the smaller bar. (b) Lithofacies B. The lower wavelet transform images are of the real seismic data.

**FIG. 3.** Conditional probabilities of the wavelet transform attribute,  $\langle \mathbf{s} \rangle$ , given the lithofacies. Histograms are the well log distributions, lines are Gaussian distributions fit to the histograms. The conditional probability of lithofacies A is shown in red and lithofacies B is shown in blue. The values of the dominate scale,  $\langle \mathbf{s} \rangle$ , expressed in the wavelet transform of the real seismic data displayed in Fig. 2 are shown as large black circles labeled as (A) lithofacies A and (B) lithofacies B.

FIGURE 1

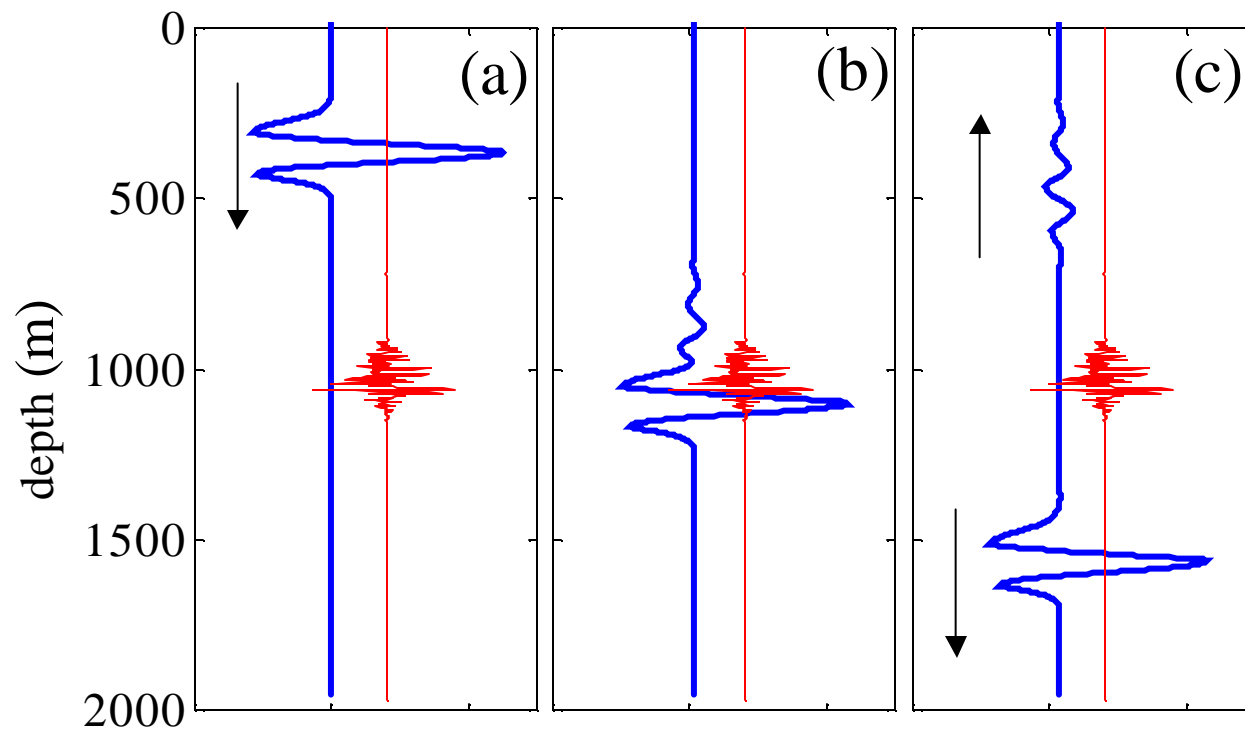


FIGURE 2

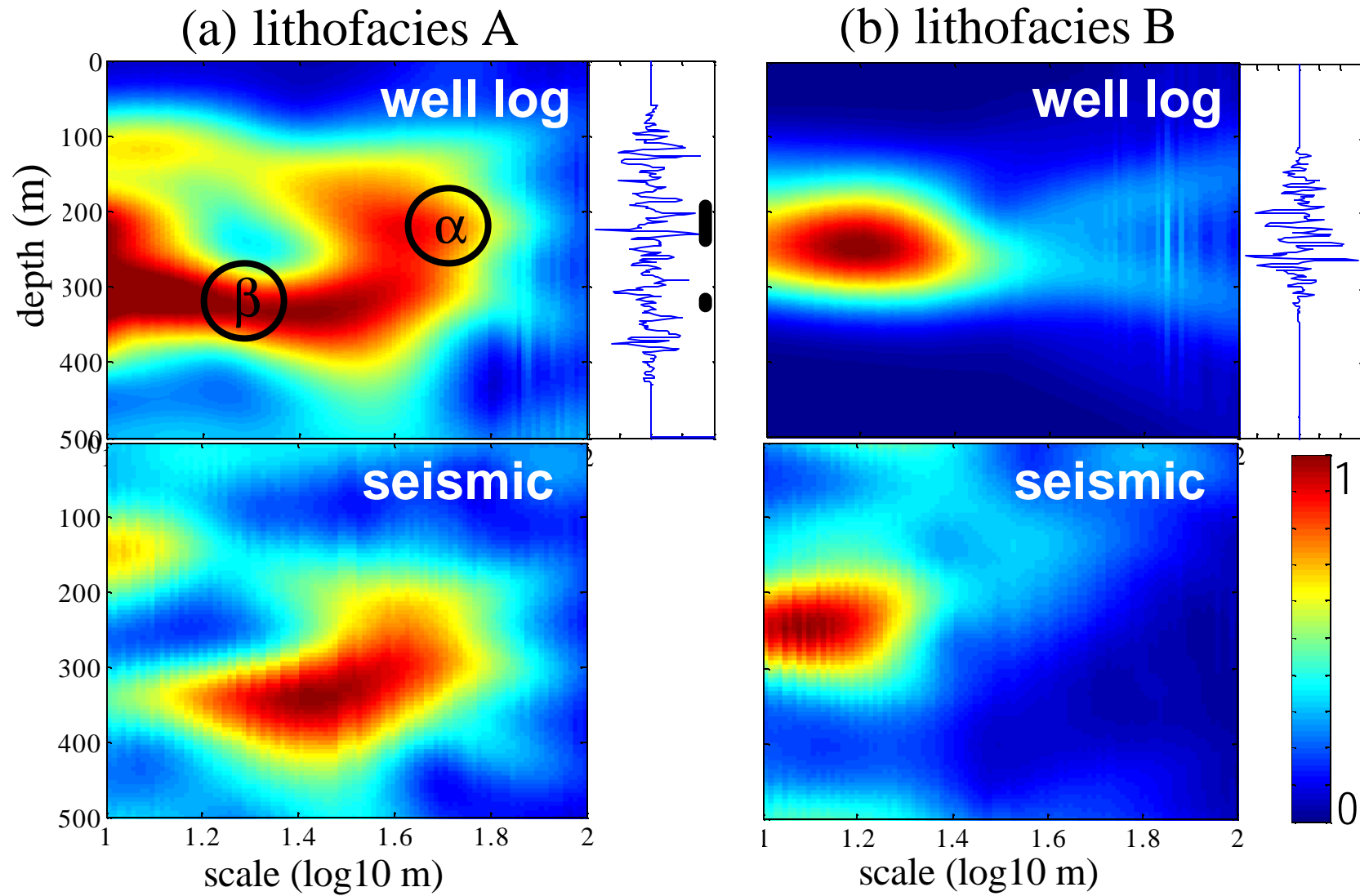


FIGURE 3

